Published in final edited form as:
*Arch Physiol Biochem*. 2010 May ; 116(2): 63–72. doi:10.3109/13813451003652997.

# MMP-2/TIMP-2/TIMP-4 versus MMP-9/TIMP-3 in Transition from Compensatory hypertrophy and angiogenesis to decompensatory heart failure*

**Srikanth Givvimani**, **Neetu Tyagi**, **Utpal Sen**, **Paras K. Mishra**, **Natia Qipshidze**, **Charu Munjal**, **Jonathan C. Vacek**, **Oluwasegun A. Abe**, and **Suresh C. Tyagi**
Department of Physiology and Biophysics, University of Louisville School of Medicine, Louisville, Kentucky-40202

## Abstract

Although matrix metalloproteinase (MMPs) and tissue inhibitor of metalloproteinase (TIMPs) play vital role in tumor angiogenesis and TIMP-3 caused apoptosis, their role in cardiac angiogenesis is unknown. Interestingly, a disruption of coordinated cardiac hypertrophy and angiogenesis contributed to the transition to heart failure, however, the proteolytic and anti-angiogenic mechanisms of transition from compensatory hypertrophy to decompensatory heart failure were unclear. We hypothesized that after an aortic stenosis MMP-2 released angiogenic factors during compensatory hypertrophy and MMP-9/TIMP-3 released antiangiogenic factors causing decompensatory heart failure. To verify this hypothesis, wild type (WT) mice were studied 3 and 8 wks after aortic stenosis, created by banding the ascending aorta in WT and MMP-9−/− (MMP-9KO) mice. Cardiac function (echo, PV loops) was decreased at 8 wks after stenosis. The levels of MMP-2 (western blot) increased at 3 wks and returned to control level at 8 wks, MMP-9 increased only at 8 wks. TIMP-2 and −4 decreased at 3 and even more at 8 wks. The angiogenic VEGF increased at 3 wks and decreased at 8 wks, the antiangiogenic endostatin and angiostatin increased only at 8 wks. CD-31 positive endothelial cells were more intensely labeled at 3 wks than in sham operated or in 8 wks banded mice. Vascularization, as estimated by x-ray angiography, was increased at 3 wks and decreased at 8 wks post-banding. Although vast majority of studies were performed on control WT mice only, interestingly, MMP9-KO mice seemed to have increased vascular density 8 wks after banding. These results suggested that there was increase in MMP-2, decrease in TIMP-2 and −4, increase in angiogenic factors and vascularization in compensatory hearts. However, in decompensatory hearts there was increase in MMP-9, TIMP-3, endostatin, angiostatin and vascular rarefaction.

### Keywords

Vasculogenesis; endothelial; endostatin; angiostatin; VEGF; capillary rarefaction; aortic banding; TAC; x-ray angiography

## Introduction

Major risk factors leading to heart failure are myocardial infarction, ischemia, chronic pressure overload such as systemic hypertension and valvular diseases. During compensatory phase,

*A part of this study was supported by NIH grants: HL-71010, HL-74185; and HL-88012.

Address correspondence to: Suresh C Tyagi PhD, Department of Physiology & Biophysics, University of Louisville School of Medicine, 500 South Preston Street, Louisville, KY 40202 Phone: 502-852-3381, Fax: 502-852-6239, s0tyag01@louisville.edu.

heart under goes ventricular remodeling and hypertrophy (McMurray & Pfeffer, 2005). However, sustained overload resulted in decompensation and end stage heart failure (Frey & Olson, 2003). It was reported that during cardiac hypertrophy, an imbalance in the ratio of capillary bed to the cardiomyocytes resulted in hypoxia, which induced hypoxia-inducible factors (Roberts & Wearn, 1941) and stimulated the release of pro-angiogenic factors, such as vascular endothelial growth factor (VEGF) (Tomanek, 1990). VEGF is a highly potent angiogenic factor that promoted endothelial cell proliferation, migration, extracellular matrix (ECM) remodeling and capillary formation (Ferrara & Davis-Smyth, 1997). These cellular events are essential process of angiogenesis that is favored by the increase in production of VEGF and simultaneous decrease in anti-angiogenic factors, such as endostatin and angiostatin (Norrby, 2006). Endogenously angiogenic factors like VEGF and FGF (Fibroblast growth factor) and anti–angiogenic factors like angiostatin and endostatin regulated the process of angiogenesis through activation of matrix metalloproteinases (MMPs, Friehs et al, 2006; Sang, 1998).

A study reported that the transition from compensatory hypertrophy to decompensatory heart failure was regulated by discoordination of angiogenesis and hypertrophy during heart failure (Shiojima et al, 2005). The anti-angiogenic factors angiostatin and endostatin were derived from plasminogen and type XVIII collagen, respectively. Studies on cancer research had shown that the expression of anti-angiogenic factors angiostatin and endostatin significantly inhibited tumor growth and vascularity in in vivo models by down regulation of VEGF expression at both mRNA and protein levels (Hajitou et al, 2002). Systemic administration of recombinant angiostatin and endostatin in tumor models had also been shown tumor regression by inhibiting angiogenesis (Hajitou et al, 2002). In another study on wound healing, endostatin had been shown to suppress ischemia induced neo-vascularization (Dobryansky et al, 2004) and mediated its anti-angiogenic actions by inhibiting the function of pro-angiogenic molecule, such as VEGF receptor (Kim et al, 2002) and activation of MMP (Kim et al, 2000). Alterations in cardiac gene expression during the transition from stable hypertrophy to heart failure elicited marked upregulation of genes ecoding ECM (Boluyt et al, 1994; Ding et al, 1999). MMP-2 is constitutively expressed, and released growth factors from the matrix during constitutive remodeling/hypetrophy/angiogenesis (Tyagi, 1997). MMP-9 is induced in heart failure (Tyagi et al, 1996) and generated collagen-matrix fragments; such as endostatin and angiostatin (Sodha et al, 2009). Tissue inhibitor of metalloproteinase-1 (TIMP-1) induced fibrosis (Lindsey et al, 2002). TIMP-2 induced cell proliferation (Lovelock et al, 2005). TIMP-3 induced apoptosis (Baker et al, 1998). TIMP-4, a cardiac specific TIMP, induced apoptosis in transformed cells, had no effect on normal cells (Tummalapalli et al, 2001). While role of pro-angiogenic and anti-angiogenic factors in the process of neo-vascularization is known; the differential role of these factors during transition from compensatory cardiac hypertrophy to decompensatory heart failure remains obscure. The hypothesis was that MMP-2 released angiogenic factors during compensatory hypertrophy and MMP-9/TIMP-3 released antiangiogenic factors causing decompensatory heart failure.

## Materials and methods

### Animals

Wild type (WT, C57BL6/J) and MMP-9−/− (MMP-9KO) mice were obtained from Jackson Laboratories (Bar Harbor, Maine), housed in the animal care facility with access to water and standard chow. All animals were 12 weeks (wks) old and between 26–30 grams. All animal procedures were performed in accordance with National Institute of Health guide lines for animal research and were reviewed and approved by the Institute Animal Care and use Committee of University of Louisville.

### Pressure overload animal model

Under pentobarbital anesthesia, animals were intubated and ventilated. A left parasternal thoracotomy was performed and the ascending aorta is identified and dissected. Banding of the ascending aorta was done by placing a 26 g needle on the anterior surface of aorta and a 6-0 silk suture was then ligated around the aorta and the needle, and needle quickly removed resulting in constriction of aorta to create pressure overload on the heart (Ding et al, 1999). The thoracotomy was then closed in layers using 6-0 vicryl and 5-0 silk sutures for skin. Post operatively all animals received ketoprofen analgesia for 48 hours. Sham animals underwent similar procedure except banding of aorta. To perform a longitudinal study, starting at time zero, all experimental results were compared with sham-op mice at the same time post-surgery. We compared 3 and 8 wks post-op mice to their controls. We included 2 groups of sham-operated mice, one studied at 3 and the other at 8 wks. The 5 mice/group was used.

### Left ventricular weight and body weight ratio (LV Wt/BW)

Animals were euthanized according to the IACUC protocol and the heart was excised, rinsed in PBS (phosphate buffer saline) and right and left ventricles were separated. Ratio of left ventricular weight and body weight was measured and represented in bar diagram.

### Antibodies & Reagents

The following primary antibodies were used for protein analysis: rabbit polyclonal anti-angiostatin, mouse monoclonal anti-endostatin, rabbit polyclonal MMP-2, and rabbit polyclonal MMP-9. These antibodies were purchased from abcam (Cambridge, MA). Rabbit polyclonal antibody against VEGF(A-20), rabbit polyclonal antibody against TIMP-2, −3, and TIMP-4, and HRP-conjugated secondary antibodies were from Santa Cruz Biotechnology (Santa Cruz, CA). Mouse monoclonal anti-GAPDH and all analytical reagents were from Sigma-Aldrich (St. Louis, MO).

### Western blot analysis

Western blot analysis heart tissue from experimental groups was harvested and washed thoroughly in PBS and snap-frozen in liquid nitrogen. Protein extraction was done using 1X RIPA buffer (Tris-HCl 50mM, pH7.4; NP-40 1%; Na-deoxycholate 0.25%; NaCl 150 mM; EDTA 1 mM; PMSF 1 mM; Na3VO4 1 mM; NaF 1 mM; protease inhibitor cocktail 1 μg/ml). Estimation of protein was done by Bradford method (Bio-Rad, Hercules, CA). 10–25 μg of protein was fractionated by SDS-PAGE and transferred onto PVDF membrane (BioRad, Hercules, CA) by wet transfer method. The transferred proteins were processed for immunodetection of specific antigens. Briefly, non-specific sites were blocked with 5% nonfat dry milk in TBS-T (50mM Tris-HCl, 150mM NaCl, 0.1% Tween- 20, pH 7.4) for 1h at room temperature. The blot was then incubated with appropriate primary antibody in blocking solution according to the supplier's specific instructions. The blots were washed with TBS-T (3times, 10min each) and incubated with appropriate HRP- conjugated secondary antibody for 1h at room temperature. After washing, ECL Plus substrate (Amersham Biosciences, Pittsburgh, PA) was applied to the blot for 1min. The blot was developed using X-ray film (RPI Corp, Inc., Mount Prospect, IL) with a Kodak 2000A developer (Eastman Kodak, Rochester, NY). The blots were stripped and re-probed with GAPDH. The immunoreactive bands were scanned and densitometricaly analyzed Un-Scan-It software (Silk Scientific, Orem, UT).

### Echocardiography

Two dimensional transthoracic echocardiography images of left ventricle from a four chambered apical view were taken with a phased-array echocardiography (SONOS 1500 or 2500; Hewlett-Packard, Inc.) and a 12.5-MHz transducer in anesthetized mice at baseline, 3

and 8 wks groups. Animals were given Tri-bromo ethanol anaesthesia (TBE). The use of tri-bromo-ethanol has minimal effect on cardiovascular function (Papaioannou & Fox, 1993). The mouse was depilated and placed on a heating pad to maintain body temperature. Cardiac function, LVIDd (left ventricular internal dimension in diastole), LVIDs (left ventricular internal dimension in systole), LVPWD (left ventricular posterior wall dimension), and Left ventricular fractional shortening % (%FS) were assessed.

### Histological analysis of cardiac sections

Frozen sections were cut at 8μm thickness using cryocut 1800 (Reichert-Jung). Cryosections were placed on superfrost plus microscope slides and air dried. Histological analysis was done in all three groups using mason's trichrome blue staining for detection of fibrosis, hematoxylin and eosin (H & E) staining for overall morphology.

### Immunohistochemistry

Immunohistochemistry was performed on 5 μm thick frozen sections of the heart using standard immunohistochemistry (IHC) protocol. Anti-Endostatin (Abcam) and anti-TIMP-2, secondarily conjugated with Texas Red (Chemicon International, St. Charles, MO) were used for immunodetection of these two proteins, respectively. Anti-PECAM-1 (CD31) clone-390, secondarily conjugated with FITC (Chemicon international, St.Charles, Missouri) was used to detect collateral density of micro-vessels.

### Coronary Angiograms

Barium sulfate contrast coronary angiograms were done on ex-vivo hearts to show the variability in vascular density of the all three groups of mice. Barium sulphate was mixed in 5.5 pH buffer and perfused into ex vivo heart at a constant flow rate and x-ray angiograms were taken with KODAK MM4000 mm with x-ray source.

### Pressure volume loop study (P-V loop)

Using standard Millar protocol, after doing two point calibration, steady state P-V loops were recorded followed by saline bolus and cuvette calibration for the conversion of RVU (relative volume units ) to μL. Hemodynamic parameters obtained were analyzed by PVAN software. The results were used to substantiate echocardiography findings.

**Statistical analysis—**All data were expressed as mean ± SE. Data were analyzed using a one-way analysis of variance to test for treatment effects, and differences between groups were determined using post hoc t-test. The level of significance was accepted at $p<0.05$.

## Results

**Echocardiographic data** showed increased septal and left ventricular posterior wall thickness during 3 wks post aortic banding (Figure 1). The fractional shortening was decreased at 8 wks aortic banding as compared to sham and/or 3 wks aortic banding. Also LVIDd (left ventricular internal dimension in diastole) increased during 3 wks aortic banding and LVPWd (Left ventricular posterior wall thickness in diastole) increased in 8 wks aortic banding as compared to sham controls. Interestingly, the left ventricular chamber size was increased at 8 wks aortic banding, suggesting dilated heart. The increase in ventricular wall thickness in 3 wks aortic banding suggested LV hypertrophy (Figure 1). These data elicited transition from compensatory phase at 3 wks to decompensatory heart failure at 8 wks aortic banding.

**Pressure-Volume relationship data** revealed that the contractility of the left ventricle decreased during 8 wks of aortic banding in comparison to sham control, depicting as shift in

pressure-volume (P-V) loops to right (Figure 2). This is further supported by quantitative data obtained showing a decrease in ejection fraction and stroke volume at 8 wks aortic banding. Also end systolic volume increased in 8 wks mice in comparison to sham controls (Figure 2). The shift of loop towards right in 8 wks aortic banding mice suggested a decrease in contractility as compared to sham.

**Gravimetric data** revealed increase in LV weight/body weight ratio at 3 wks aortic banding and stayed elevated at 8 wks of aortic banding (Figure 3). These data suggested compensatory hypertrophy at 3 wks and decompensatory heart failure at 8 wks of aortic banding. To determine interestitial and pericapillary fibrosis, trichrome-blue collagen hhistological staining was performed. Although basal level of collagen was detected in the sham group (Figure 4), there was collagen deposition at 3 wks post aortic banding. The fibrosis was abundant at both the interstitial and epicardial regions of the hearts from 8 wks aortic banding mice.

## MMPs/TIMPs axis and angiogenic/antiangiogenic factors in compensatory to decompensatory heart failure

The expression of MMP-9 showed very little increase at 3 wks aortic banding as compared to sham (Figure 5). However, the expression was robust at 8 wks post banding as compared to either sham and/or 3 wks banding. Contrary to MMP-9, MMP2 was increased at 3 wks, although active MMP2 was unchanged. Interestingly, this increase was almost normalized at 8 wks post aortic banding (Figure 5). These results suggested a differential role of MMP-2 versus MMP-9 during transition from compensatory cardiac hypertrophy to decompensatory heart failure.

The expression of TIMP-2 is decreased at 3 and 8 wks, compared to sham control (Figure 6). However, a gradual decrease in TIMP-4 expression was observed from 3 wks to 8 wks post aortic banding (Figure 6). This suggested the decrease in TIMP-2 and TIMP-4 levels in decompensatory heart failure.

Since TIMP-3 instigates apoptosis, we measured the levels of TIMP-3 along with MMP-2, in situ. Although MMP-2 and TIMP-3 co-localized, contrary to TIMP-2/TIMP-4, the immunohistochemistry data revealed increase in TIMP-3 levels at 3 wks, however, interestingly, at 8 wks of aortic banding hearts TIMP-3 was robust (Figure 7). The in situ data also revealed that MMP-2 was elevated during 3 wks with tendency to decrease at 8 wks of aortic banding as compared to sham (Figure 7).

Since MMP-2 released growth factors from the matrix and promotes angiogenesis, we measured the levels of angiogenic VEGF and anti-angiogenic (endostatin and angiostatin) levels. The levels of VEGF-A was increased in 3 wks group as compared to sham controls (Figure 8). However, the expression of VEGF-A was diminished during 8 wks post aortic banding, suggesting the decrease in angiogenic factors in decompensatory heart failure (Figure 8). The expression of anti–angiogenic factors like endostatin and angiostatin increased significantly at 8 wks post aortic banding as compared to sham and/or 3 wks banding (Figure 8). The increase in expression of endostatin at 8 wks aortic banding was further evidenced by immuno histochemical staining (Figure 9).

## Angiogenesis/vasculogenesis

The CD31 staining (an endothelial cell marker) showed increased density of endothelial cells during 3 wks as compared sham and 8 wks aortic banding groups, suggesting increased endothelial cell density (Figure 10). Interesting, staining with CD31 also visualized the capillaries, the endothelial cells density in the capillaries density was also increased at 3 wks as compared to sham or 8 wks aortic banding.

To corroborate CD-31 endothelial/capillary data with vasculogenesis, we performed in vivo real-time soft-tissue x-ray angiography using barium as contrasting agent. The angiographic data showed increased in vascular density at 3 wks aortic banding; whereas capillary rarefaction was observed at 8 wks post aortic banding (Figure 11). To determine the role of MMP-9 as inducers of anti-angiogenic factors (endostatin and angiostatin), we created aortic banding in MMP-9−/− (MMP-9KO) mice. The results suggested increase in vascular density in MMP-9KO after 8 wks aortic banding as compared to sham controls (Figure 11).

## Discussion

Systemic hypertension causing left ventricular pressure overload is one of the leading risk factor of cardiac hypertrophy that eventually leads to heart failure. These hypertrophied hearts exhibited contractile dysfunction, dilation of the ventricular wall and increased wall thickness (Allard et al, 1994). In the normal human heart, after acute ischemic injury, LV wall stress increased, whereas wall thickness and ejection fraction decreased. To compensate for the load the entire myocardium undergoes compensatory hypertrophy/remodeling i.e. enlargement of the muscle tissue that remodeled the entire chamber. While during compensatory response, the ejection fraction and wall thickness were increased, in decompensatory heart failure, ejection fraction and wall thickness decreased significantly (Pouleur et al, 1993). Our studies suggested that there was increase in MMP-2, decrease in TIMP-2 and −4, increase in angiogenic factors and vascularization in compensatory hearts. However, in decompensatory hearts there was increase in MMP-9, TIMP-3, endostatin, angiostatin, and vascular rarefaction. The increased expression of VEGF-A during 3 wks post aortic banding showed the importance of angiogenesis during hypertrophy. There was an increase in the expression of angiostatin and endostatin in the 8 wks post aortic banding. These data suggested that the higher levels of angiogenic factors provide impulse for cardiac compensation while up-regulation of anti-angiogenic factors promoted decompensatory heart failure.

During angiogenesis, increased expression of VEGF is associated with simultaneous decrease in anti-angiogenic factors, such as endostatin and angiostatin. Endostatin is derived from collagen XVIII, that had been shown to inhibit angiogenesis (O'Reilly et al, 1997) and endostatin induces endothelial cell apoptosis (Dhanabal et al, 1999; Felbor et al, 2000). Angiostatin is a cleavage product of plasminogen. Angiostatin has been reported to induce endothelial cell death (Tarui et al, 2001), inhibits endothelial cell proliferation (Sharma et al, 2004), migration and tube formation (Troyanovsky et al, 2001). Our study demonstrated that increased capillary density, as evidenced by increased endothelial cell population, was observed during 3 wks of aortic banding, and this was supported by the evidence of upregulated VEGF-2A and basal level of endostatin and angiostatin expression. Conversely, during decompensatory heart failure (8 wks aortic banding), VEGF-2A was diminished and up regulation of endostatin and angiostatin was observed resulting in decrease of capillary density.

The endogenous inhibitor of MMP, TIMPs inhibits MMPs activity; therefore, the balance of MMPs/TIMPs is very important in order to maintain normal physiological matrix architecture (Tyagi, 1997). MMP-2 and 9 both are able to cleave collagen and play a major role in ECM remodeling. During cardiac hypertrophy and chronic heart failure, the imbalance of MMPs/TIMPs caused changes in matrix composition, resulting in cardiac fibrosis. TIMP-2 and TIMP-4 inhibit both MMP-2, and −9, and therefore, decrease in TIMP-2 and TIMP-4 augments MMP-2 and −9 activities that promote cardiac fibrosis. The results of this study showed that increased fibrosis was observed at 8 wks post aortic banding. This was consistent with up regulation of MMP-9. Interestingly, an up regulation of MMP-2 was observed at 3 wks and a down regulation of MMP-2 was observed in 8 wks aortic banding. This suggested possible differential regulation of these two MMPs by TIMP-2 and TIMP-4 during compensatory cardiac hypertrophy leading to decompensatory heart failure. Interestingly, TIMP-3 was

increased at 3 wks and continued to be increased at 8 wks aortic banding. This may suggest TIMP-3 associated cell death (Baker et a, 1998).

In conclusion, our study showed that pressure-overload cardiac hypertrophy was compensated with increased angiogenesis and MMP-2 whereas decompensatory heart failure was accompanied with increase in MMP-9 and TIMP-3, resulted in non-specific collagen cleavage and upregulation of potent antiangiogenic factors that eventually led to heart failure (Figure 12). The novelty of this study was the mechanistic disconnect between angiogenesis/hypertrophy in compensatory heart to anti-angiogenesis/hypertrophy in de-compensatory heart failure.

### Limitations

Although we do not have direct connection as to whether the MMP-2 releases angiogenic factors and MMP-9/TIMP-3 releases antiangiogenic factors in stressed hearts, we show data that the levels of MMP-2 and −9, TIMP-2, −3 and −4, VEGF, angiostatin and endostatin are modified in the direction suggested by the hypothesis, and may elicit a causal relationship. With immuno-labeling, presumably, we detected both inactive Pro and active MMP-2. Also, the histochemical data shown in Figure 7 detected total active and pro MMP-2. However, without a change in active MMP-2, we can not infer specifically that MMP-2 elevation was responsible for the pro-angiogenic changes at 3 wks. Although it may be unclear whether we really estimated the vascular density by measuring the black pixels, and because the blood flow in coronary arteries was pulsatile, however, we have taken the images of the heart in diastole using KCl at the same time of cardiac cycle. The shadowed triangles in the center of sham, 8 wks and MMP9 KO were due to cavity variation, we avoid these triangles in counts. In MMP-9KO mice, the amelioration of cardiac dysfunction in many pathophysiology were already demonstrated (Ducharme et al, 2000;Camp et al, 2003;Lindsey et al, 2006), here we showed that in the MMP-9 KO mice anti-vasculogenesis was mitigated (Figure 11).

## References

Allard MF, Flint JD, English JC, Henning SL, Salamanca MC, Kamimura CT, English DR. Calcium overload during reperfusion is accelerated in isolated hypertrophied rat hearts. J Mol Cell Cardiol 1994;26:1551–1563. [PubMed: 7731050]

Baker AH, Zaltsman AB, George SJ, Newby AC. Divergent effects of tissue inhibitor of metalloproteinase-1, −2, or −3 overexpression on rat vascular smooth muscle cell invasion, proliferation, and death in vitro. TIMP-3 promotes apoptosis. J Clin Invest 1998 Mar 15;101(6):1478–87. [PubMed: 9502791]

Boluyt MO, O'Neill L, Meredith AL, Bing OH, Brooks WW, Conrad CH, Crow MT, Lakatta EG. Alterations in cardiac gene expression during the transition from stable hypertrophy to heart failure. Marked upregulation of genes encoding extracellular matrix components. Circ Res 1994;75(1):23–32. [PubMed: 8013079]

Camp TM, Tyagi SC, Senior RM, Hayden MR, Tyagi SC. Gelatinase B (MMP-9) an apoptotic factor in diabetic transgenic mice. Diabetologia 2003;46(10):1438–1445. [PubMed: 12928773]

Dhanabal M, Ramchandran R, Waterman MJ, Lu H, Knebelmann B, Segal M, Sukhatme VP. Endostatin induces endothelial cell apoptosis. J Biol Chem 1999;274:11721–11726. [PubMed: 10206987]

Ding B, Price RL, Borg TK, Weinberg EO, Halloran PF, Lorell BH. Pressure overload induces severe hypertrophy in mice treated with cyclosporine, an inhibitor of calcineurin. Circ Res 1999;84:729–734. [PubMed: 10189361]

Dobryansky M, Galiano RD, Cetrulo CL Jr, Bhatt KA, Michaels J, Ashinoff R, Levine JP, Gurtner GC. Endostatin inhibits ischemia-induced neovascularization and increases ischemic tissue loss. Ann Plast Surg 2004;52:512–518. [PubMed: 15096942]

Ducharme A, Frantz S, Aikawa M, Rabkin E, Lindsey M, Rohde LE, Schoen FJ, Kelly RA, Werb Z, Libby P, Lee RT. Targeted deletion of matrix metalloproteinase-9 attenuates left ventricular

enlargement and collagen accumulation after experimental myocardial infarction. J Clin Invest 2000 Jul;106(1):55–62. [PubMed: 10880048]

Felbor U, Dreier L, Bryant RA, Ploegh HL, Olsen BR, Mothes W. Secreted cathepsin L generates endostatin from collagen XVIII. EMBO J 2000;19:1187–1194. [PubMed: 10716919]

Ferrara N, Davis-Smyth T. The biology of vascular endothelial growth factor. Endocr Rev 1997;18:4–25. [PubMed: 9034784]

Frey N, Olson EN. Cardiac hypertrophy: the good, the bad, and the ugly. Annu Rev Physiol 2003;65:45–79. [PubMed: 12524460]

Friehs I, Margossian RE, Moran AM, Cao-Danh H, Moses MA, del Nido PJ. Vascular endothelial growth factor delays onset of failure in pressure-overload hypertrophy through matrix metalloproteinase activation and angiogenesis. Basic Res Cardiol 2006;101(3):204–13. [PubMed: 16369727]

Hajitou A, Grignet C, Devy L, Berndt S, Blacher S, Deroanne CF, Bajou K, Fong T, Chiang Y, Foidart JM, Noel A. The antitumoral effect of endostatin and angiostatin is associated with a down-regulation of vascular endothelial growth factor expression in tumor cells. FASEB J 2002;16:1802–1804. [PubMed: 12354694]

Kim YM, Hwang S, Pyun BJ, Kim TY, Lee ST, Gho YS, Kwon YG. Endostatin blocks vascular endothelial growth factor-mediated signaling via direct interaction with KDR/Flk-1. J Biol Chem 2002;277:27872–27879. [PubMed: 12029087]

Kim YM, Jang JW, Lee OH, Yeon J, Choi EY, Kim KW, Lee ST, Kwon YG. Endostatin inhibits endothelial and tumor cellular invasion by blocking the activation and catalytic activity of matrix metalloproteinase. Cancer Res 2000;60:5410–5413. [PubMed: 11034081]

Lindsey ML, Escobar GP, Dobrucki LW, Goshorn DK, Bouges S, Mingoia JT, McClister DM Jr, Su H, Gannon J, MacGillivray C, Lee RT, Sinusas AJ, Spinale FG. Matrix metalloproteinase-9 gene deletion facilitates angiogenesis after myocardial infarction. Am J Physiol Heart Circ Physiol 2006;290(1):H232–9. [PubMed: 16126817]

Lindsay ML, Maxwell P, Dunn FG. TIMP-1: a marker of left ventricular diastolic dysfunction and fibrosis in hypertension. Hypertension 2002;40:136–141. [PubMed: 12154103]

Lovelock JD, Baker AH, Gao F, Dong JF, Bergeron AL, McPheat W, Sivasubramanian N, Mann DL. Heterogeneous effects of tissue inhibitors of matrix metalloproteinases on cardiac fibroblasts. Am J Physiol Heart Circ Physiol 2005;288(2):H461–8. [PubMed: 15650153]

McMurray JV, Pfeffer MA. Heart Failure. The Lancet 2005;365(9474):1877–1889.

Norrby K. In vivo models of angiogenesis. J Cell Mol Med 2006;10:588–612. [PubMed: 16989723]

O'Reilly MS, Boehm T, Shing Y, Fukai N, Vasios G, Lane WS, Flynn E, Birkhead JR, Olsen BR, Folkman J. Endostatin: an endogenous inhibitor of angiogenesis and tumor growth. Cell 1997;88:277–285. [PubMed: 9008168]

Papaioannou VE, Fox JG. Efficacy of tribromoethanol anesthesia in mice. Lab Anim Sci 1993;43:189–192. [PubMed: 8320967]

Pouleur H, Rousseau MF, van Eyll C, Melin J, Youngblood M, Yusuf S. Cardiac mechanics during development of heart failure. SOLVD Investigators. Circulation 1993;87(5 Suppl):IV14–20. [PubMed: 8485829]

Roberts JT, Wearn JT. Quantitative changes in the capillary-muscle relationship in human hearts during normal growth and hypertrophy. Am Heart J 1941;16:617–633.

Sang QX. Complex role of matrix metalloproteinases in angiogenesis. Cell Res 1998 Sep;8(3):171–7. [PubMed: 9791730]

Sharma MR, Tuszynski GP, Sharma MC. Angiostatin-induced inhibition of endothelial cell proliferation/apoptosis is associated with the down-regulation of cell cycle regulatory protein cdk5. J Cell Biochem 2004;91:398–409. [PubMed: 14743398]

Shiojima I, Sato K, Izumiya Y, Schiekofer S, Ito M, Liao R, Colucci WS, Walsh K. Disruption of coordinated cardiac hypertrophy and angiogenesis contributes to the transition to heart failure. J Clin Invest 2005;115(8):2108–18. [PubMed: 16075055]

Sodha NR, Clements RT, Boodhwani M, Xu SH, Laham RJ, Bianchi C, Sellke FW. Endostatin and angiostatin are increased in diabetic patients with coronary artery disease and associated with impaired coronary collateral formation. Am J Physiol Heart Circ Physiol 2009;296(2):H428–34. [PubMed: 19074676]

Tarui T, Miles LA, Takada Y. Specific interaction of angiostatin with integrin alpha(v)beta(3) in endothelial cells. J Biol Chem 2001;276:39562–39568. [PubMed: 11514539]

Tomanek RJ. Response of the coronary vasculature to myocardial hypertrophy. J Am Coll Cardiol 1990;15:528–533. [PubMed: 1689327]

Troyanovsky B, Levchenko T, Mansson G, Matvijenko O, Holmgren L. Angiomotin: an angiostatin binding protein that regulates endothelial cell migration and tube formation. J Cell Biol 2001;152:1247–1254. [PubMed: 11257124]

Tummalapalli CM, Heath BJ, Tyagi SC. Tissue inhibitor of metalloproteinase-4 instigates apoptosis in transformed cardiac fibroblasts. J Cell Biochem 2001;80(4):512–21. [PubMed: 11169735]

Tyagi SC. Proteinases and myocardial extracellular matrix turnover. Mol Cell Biochem 1997;168(1–2): 1–12. [PubMed: 9062888]

Tyagi SC, Kumar SG, Haas SJ, Reddy HK, Voelker DJ, Hayden MR, Demmy TL, Schmaltz RA, Curtis JJ. Post-transcriptional regulation of extracellular matrix metalloproteinase in human heart end-stage failure secondary to ischemic cardiomyopathy. J Mol Cell Cardiol 1996;28(7):1415–28. [PubMed: 8841929]

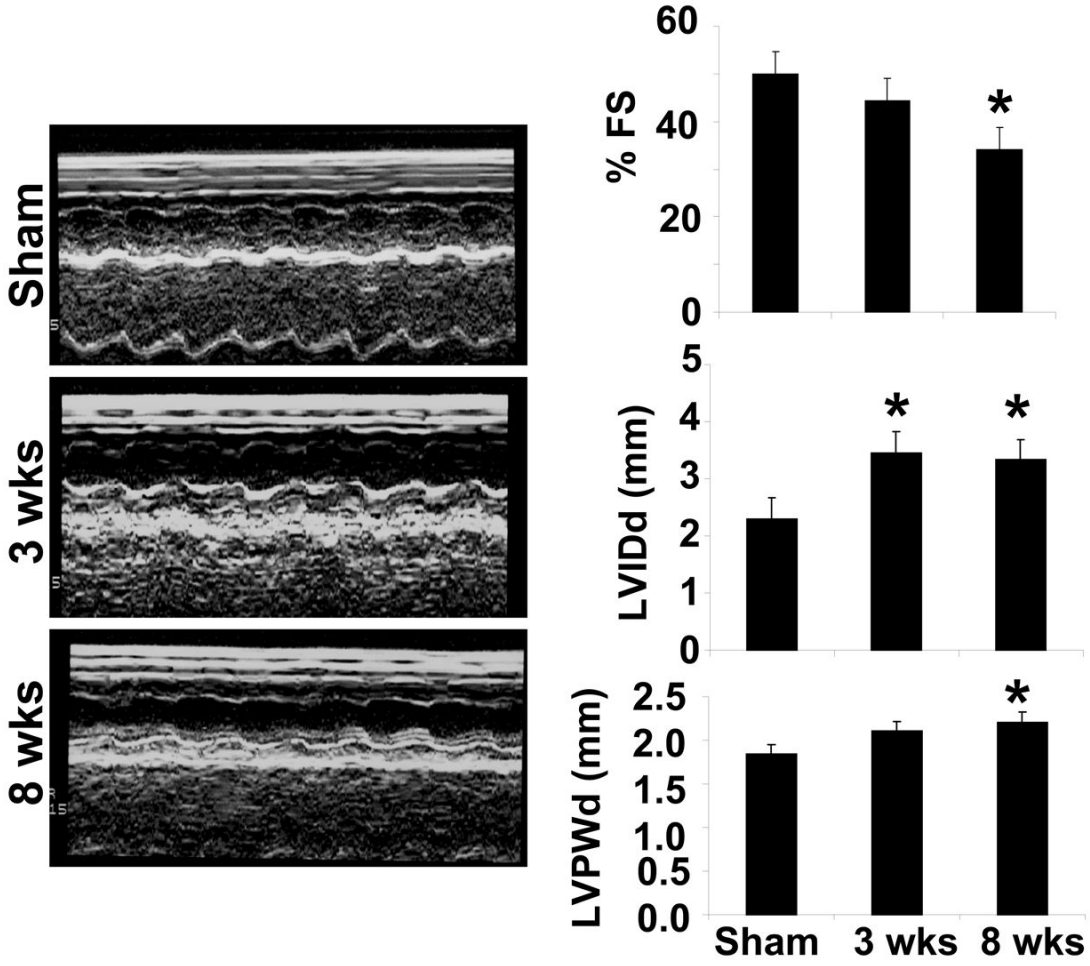


**Figure 1.**

Panels represented M-mode echocardiography of Sham (8wks), 3 wks and 8 wks after aortic banding. The bars graphs represented % fraction shortening (FS), LVIDd (left ventricular internal dimension in diastole), and LVPWd (left ventricular posterior wall dimension in diastole). *, $p<0.05$ compared with sham. All bar graphs depicted mean+SE from n=5/group

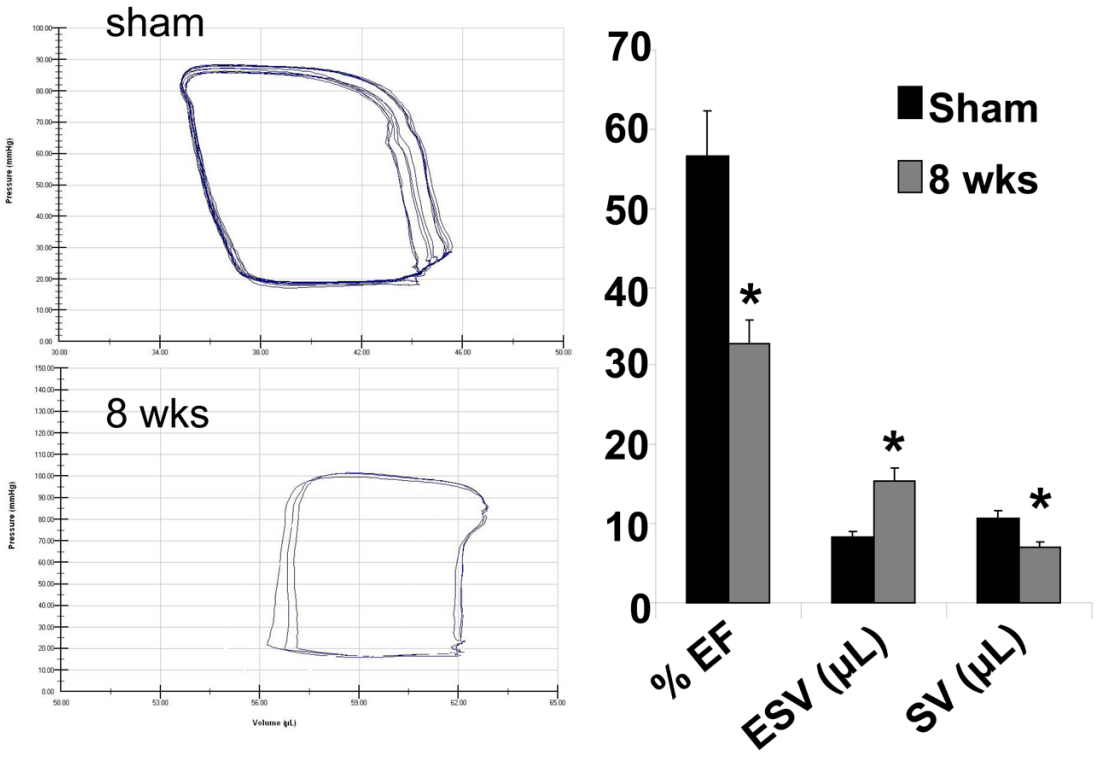


**Figure 2.**

Pressure-volume loop by Millar catheter of Sham (8wks) and 8 wks aortic banding mice: The bar graphs depict % ejection fraction (EF), ESV (End systolic stroke volume), and stroke volume (SV) in sham and 8 wks aortic banding mice. The data presented mean±SE from n=5/group *, $p<0.05$ vs sham. PV analysis in vivo is load-dependent, that changes in after load and preload after banding can influence the parameters independently of heart failure at 8 wks.

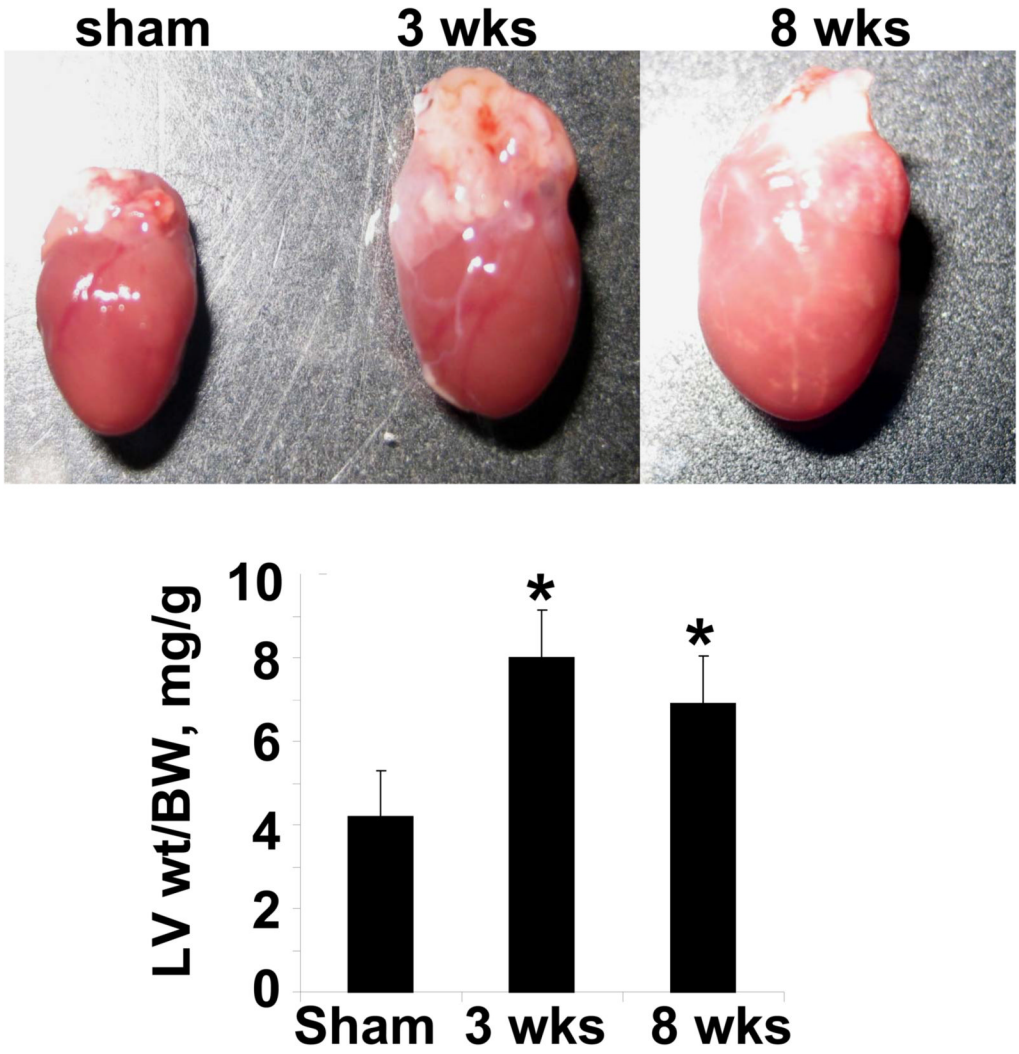


**Figure 3.**
The gross images of the whole heart of Sham (8wks), 3 wks, and 8 wks aortic banding. Hearts were cleansed in phosphate buffered saline. The left ventricle was separated. The ratio of left ventricle (LV) weight (wt) to body weight (BW) was depicted in bar graph. The data presented mean±SE, n=5/group. *, $p<0.01$ vs Sham.

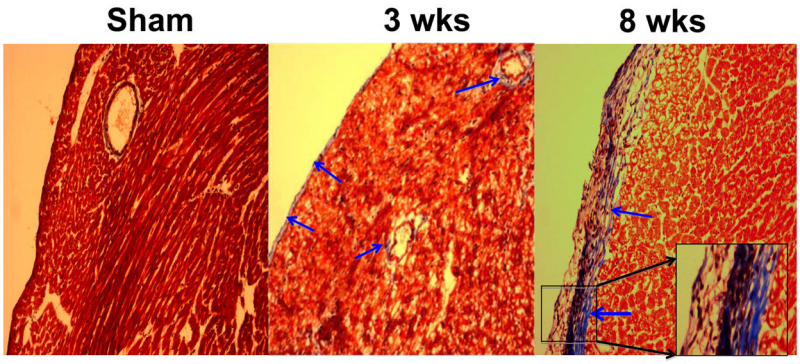


**Figure 4.**

Representative microphotographs of mason's-trichrome blue histological staining of frozen heart sections: The hearts from sham (8wks), 3 wks and 8 wks aortic banding were analyzed. Arrow indicates endocardial and pericapillary fibrosis. 20 x magnifications. The insert box, 100 x magnifications.

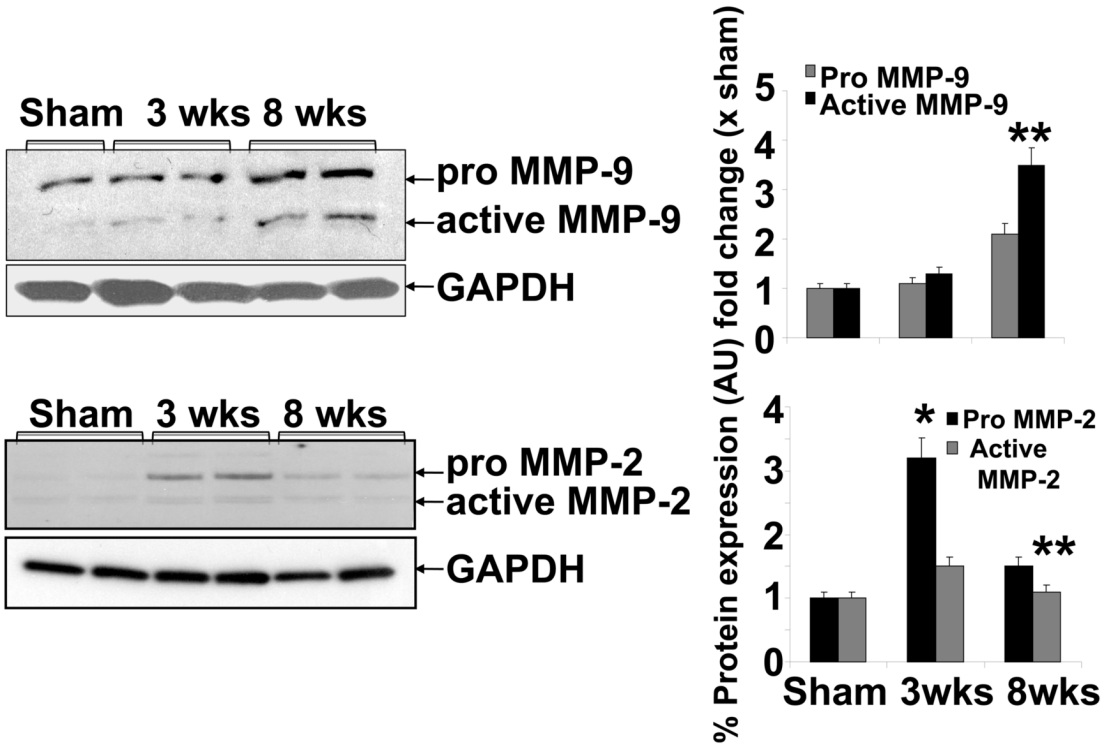


**Figure 5.**

Western blot analyses of MMP-9 and MMP-2 expression in Sham (8wks), 3 wks and 8 wks of aortic banding: Bar graphs showed densitometric analyses of MMP-9 and MMP-2 expression over sham groups (protein normalized with GAPDH). Each bar represents mean ± SE, *p<0.05 vs sham, **, compared with 3 wks, from n=5 in each group. The % protein expression on Y-axis is the protein expression calculated as fold change vs. sham.

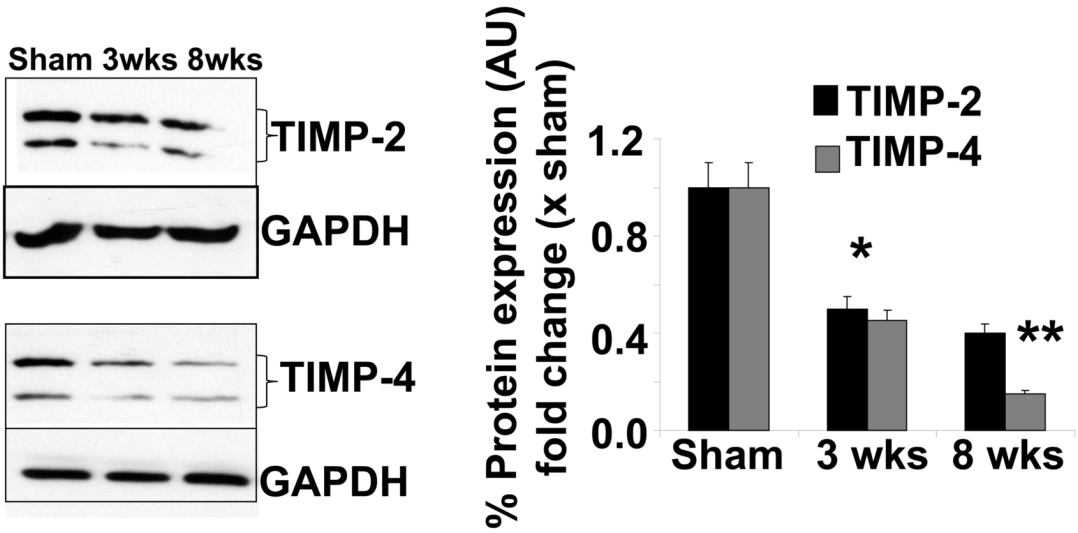


**Figure 6.**

Western blot analyses of TIMP-2 and TIMP-4 expression in Sham (8wks), 3 wks and 8 wks of aortic banding: Bar graphs showed densitometric analyses of TIMP-2 and TIMP-4 expression over sham groups (protein normalized with GAPDH). Each bar represents mean ± SE, *p<0.05 vs sham, **, compared with 3 wks, from n=5 in each group. The % protein expression on Y-axis is the protein expression calculated as fold change vs. sham.

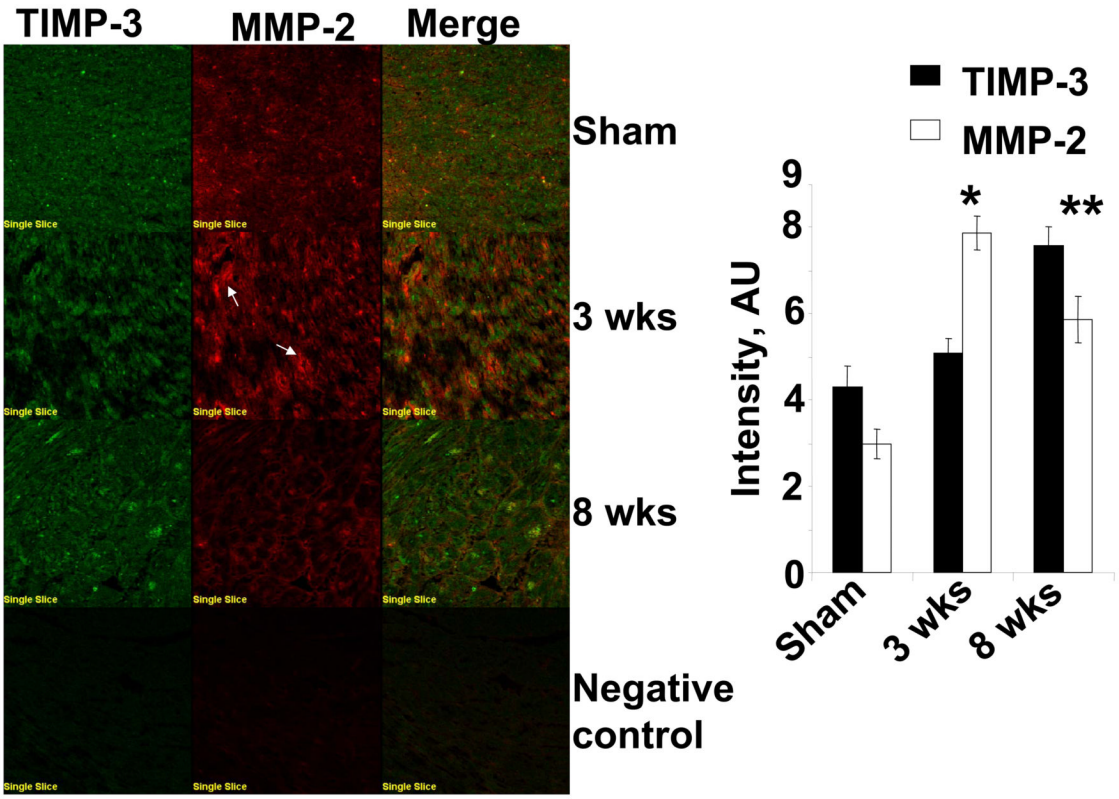


**Figure 7.**

Left ventricle immunohistochemical staining and co-localization of TIMP-3 and MMP-2: Cryocut frozen sections of (8–10 μm) were stained and secondarily conjugated with FITC for TIMP-3 and texas red for MMP-2 (white arrows indicate capillaries). The bar diagrams depicted the intensity quantification of TIMP-3 and MMP-2 by Fluoview software, in sham (8wks), 3 wks and 8 wks aortic banding. Data presented mean ± SE; *$p<0.01$ vs sham; **$p<0.05$ vs 3 wks; n=5 animals per group.

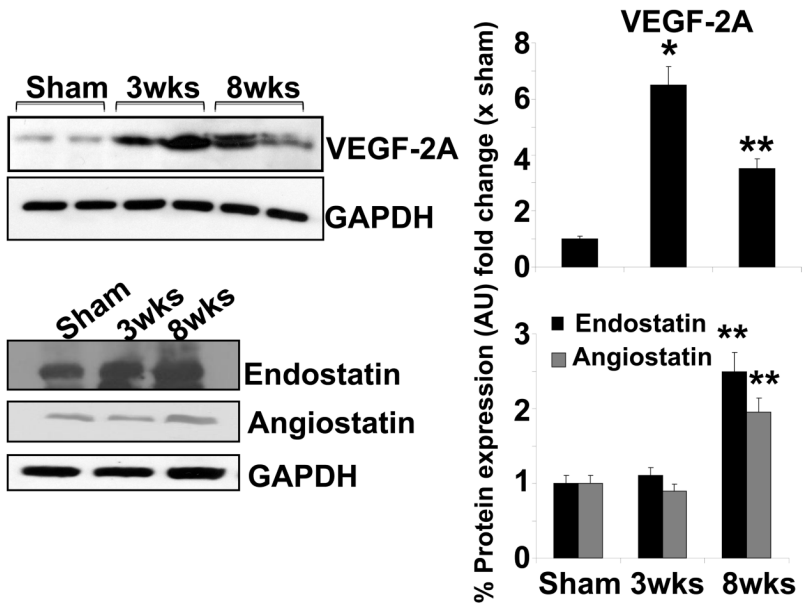


**Figure 8.**

Measurement of angiogenic and anti-angiogenic factors: Western blot analyses of VEGF-A, endostatin and angiostatin. Bar graphs showed the relative expression of VEGF-A, endostatin, and angiostatin over sham group (after normalization with GAPDH). The data presented mean ±SE, * $p<0.05$ vs sham; **, compared with 3wks. The % protein expression on Y-axis is the protein expression calculated as fold change vs. sham.

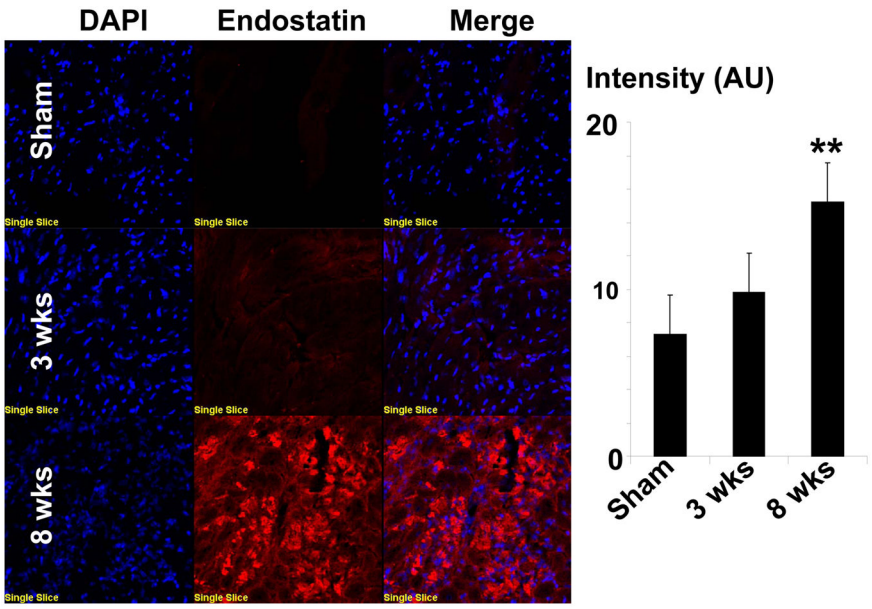


**Figure 9.**

Immunohistochemical staining of endostatin. Cryocut frozen tissue sections (5 μm) are stained with anti-endostation antibody secondarily conjugated with Texas red dye. Nuclei are stained with DAPI. Bar diagrams depicted intensity quantification by image pro-software. Each bar representative mean±SE, **p<0.05 vs sham or 3 wks, n=5 animals/group.

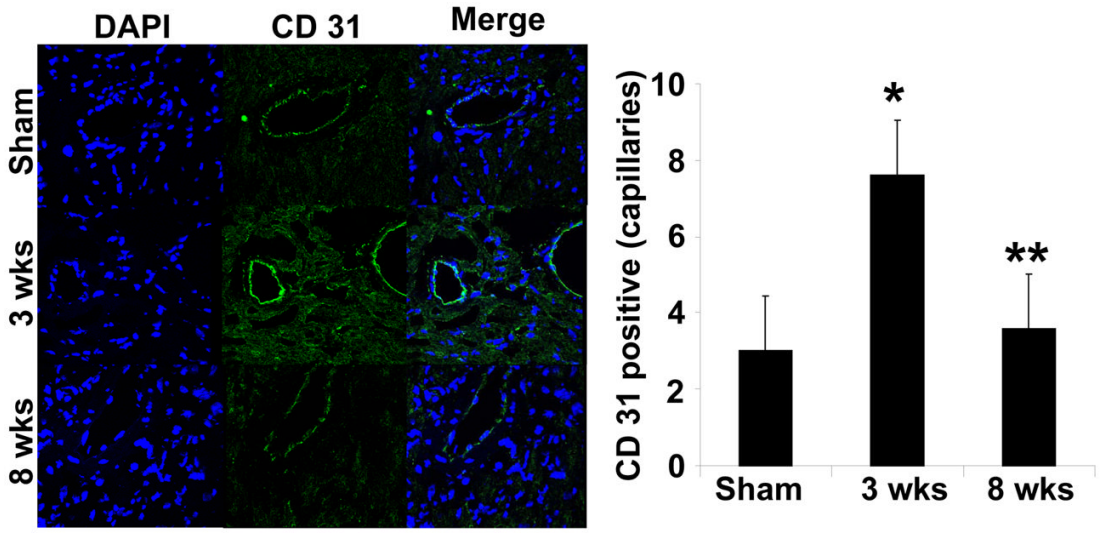


**Figure 10.**

Immunohistochemical staining with CD31 (PECAM) in sham (8wks), 3 wks and 8 wks aortic banding groups. DAPI was used for nuclear staining. The images were merged. The arrows point to capillary structure. Bar diagrams represent quantified arbitrary number of CD 31staining endothelial cell in capillaries per each field randomly selected with the help of Image-Pro software. The data presented mean±SE, n=5/group. * $p<0.01$ vs Sham; ** $p<0.05$ vs 3 wks.

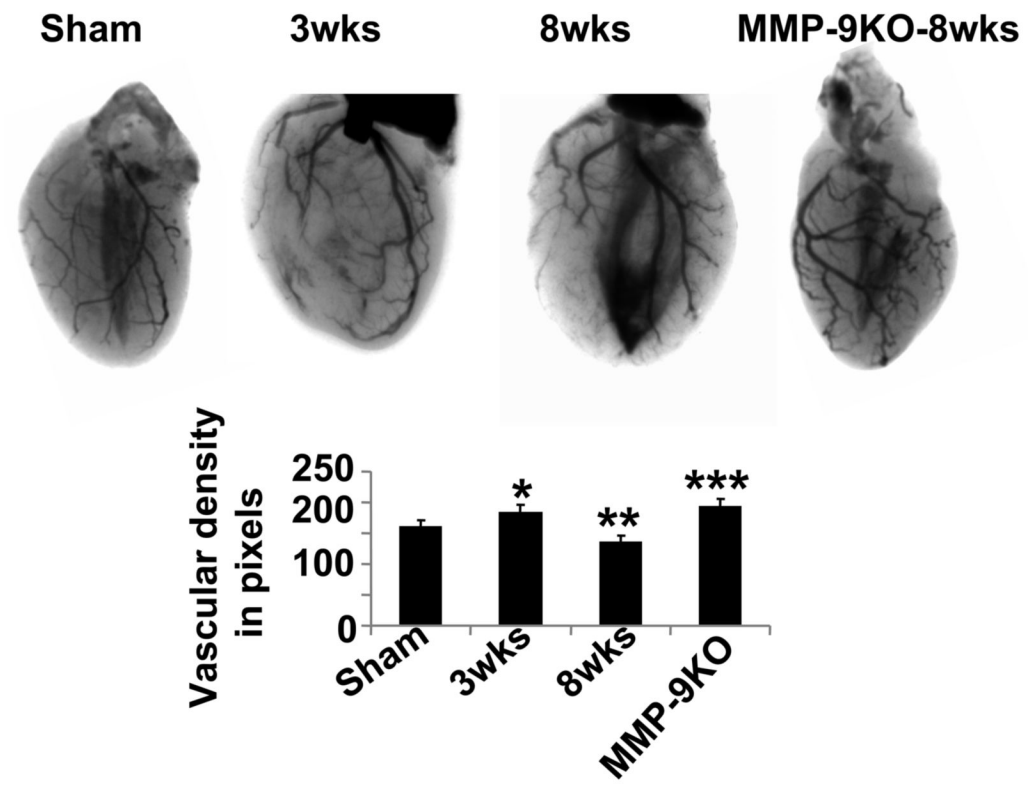


**Figure 11.**

Barium-contrast x-ray angiograms, to demonstrate gross variability in vasculature among sham (8wks), 3 wks, 8 wks and MMP-9KO (at 8 wks). In vivo hearts were perfused with Barium sulfate solution and x-ray imaging was taken with KODAK MM4000 in both in whole body and in isolated hearts. The bar diagrams depicted quantified intensity of the images from randomly chosen areas of same size, with Image-J software. The data presented mean±SE, *p<0.05 vs sham; **p<0.01 vs 3 wks; ***, compared with 8wks. n=5 animals per group.

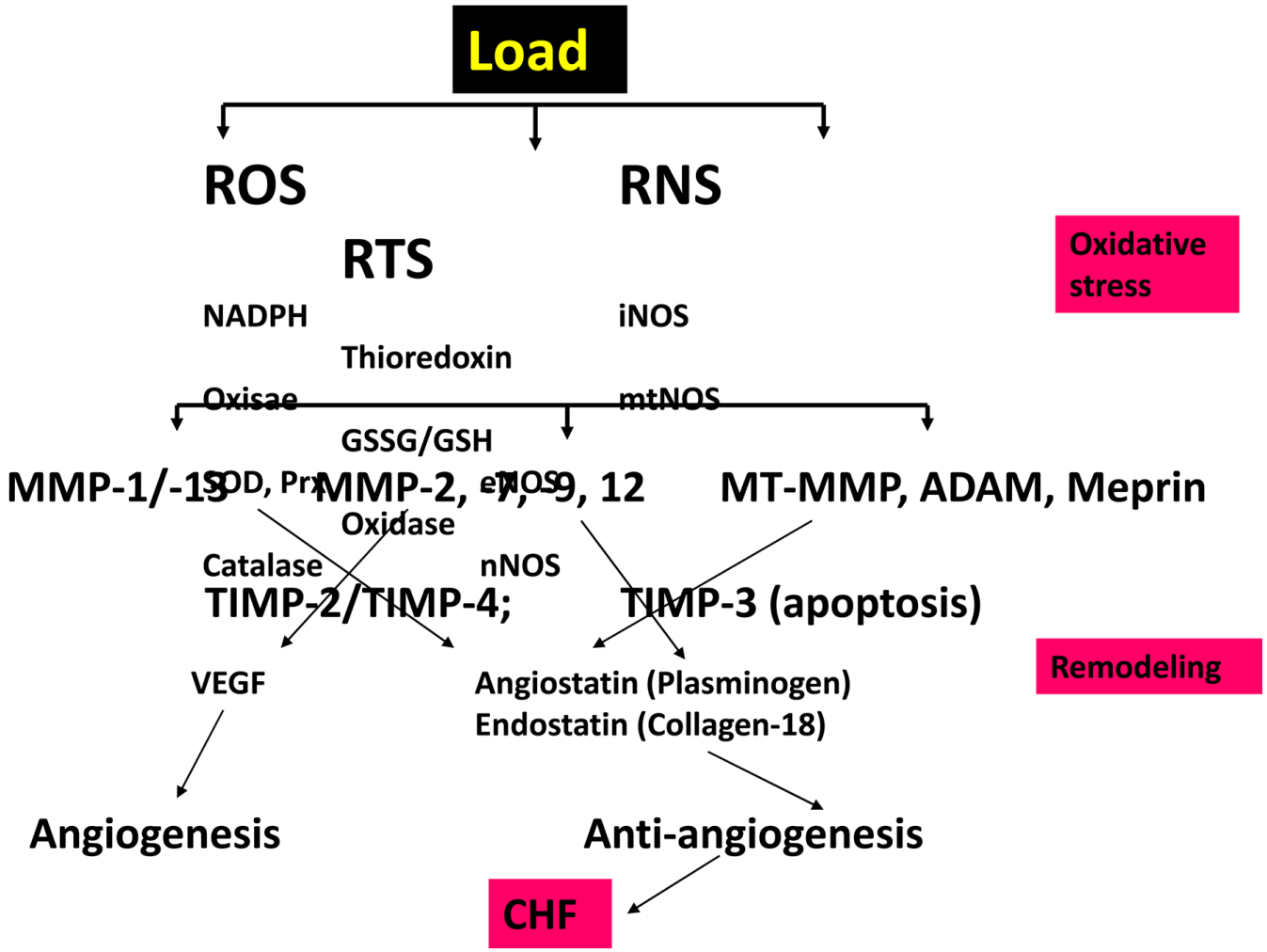


**Figure 12.**

Hypothetical presentation of latent MMP activation under chronic oxidative load condition. The imbalance in MMP/TIMP axis and remodeling, generating angiogenic, anti-angiogenic, factors, leading to apoptosis and chronic heart failure (CHF). Abbreviations: ROS, reactive oxygen species; RNS, reactive nitrogen species; RTS, reactive thiol species; NADH, nicotinamide adenine dinucleotide (reduced); SOD, superoxide dismutase; Prx, peroxiredoxin; VEGF, vascular endothelial growth factor; ADAM, a disintegrin and metalloproteinase; Meprins, metalloproteinase in renal; iNOS, inducible nitric oxide synthase; eNOS, endothelial nitric oxide synthase; GSSG/GSH, oxidized glutathione/reduced glutathione; mtMMP, mitochondrial MMP; MT-MMP, membrane type-MMP.